

Appendix 2.5BB Updated Characterization of Large-Magnitude New Madrid Seismic Zone Earthquake Model

The following description of the updated characterization of fault sources that are judged to be the sources for the 1811 and 1812 earthquake sequence and similar paleo-earthquake sequences in the NMSZ is excerpted from the Bellefonte Units 3 & 4 COLA FSAR. [Tables, Figures, and References cited in the following text is from the excerpt and are not associated with Fermi 3 citations]

2.5.2.4.4 Updated PSHA

The revisions described in Subsection 2.5.2.4.3 identified three specific elements of the EPRI-SOG evaluations that are impacted by the new information and data. The areas that require revision are: (1) the characterization of the size and rate of the more frequently occurring large magnitude New Madrid events originating on the fault system that generated the 1811-1812 earthquake sequence; (2) the characterization of the source geometry, recurrence, and magnitude of repeating large magnitude earthquakes in the Charleston region (which has only a very minor impact on the site hazard); and (3) new ground motion models for the CEUS. The modifications to the EPRI-SOG seismic hazard model to incorporate these updates are discussed in the following sections. Note that, with the exception of the repeating large magnitude New Madrid and Charleston earthquakes, the seismicity parameters defined for the EPRI seismic sources are unchanged by new data and are found, consistent with Regulatory Guide 1.208, to be appropriate for use in the updated PSHA for the BLN site.

The first two revisions incorporated sources of repeating large magnitude earthquakes at New Madrid and Charleston with return intervals of approximately 500 and 550 years, respectively, into the seismic hazard model. Ideally, the EPRI characterization of these sources should be updated to reflect the recent data. However, because of the large distance between these sources and the BLN site (> 200 mi.), what is of primary importance is the characterization of the size and frequency of the largest earthquakes. This is illustrated by the magnitude-distance deaggregation of the mean hazard from the EPRI model. Figure 2.5-258 shows the deaggregation of mean hazard at ground motion amplitudes corresponding to annual exceedance frequencies of 10⁻⁴, 10⁻⁵, and 10⁻⁶. The hazard from distances greater than 200 mi. is primarily from large earthquakes in the New Madrid source.

Subsections 2.5.2.4.4.1 and 2.5.2.4.4.2 describe the models used for repeating large magnitude earthquakes in the New Madrid and Charleston seismic zones, respectively. These models include the recurrence rates and magnitudes. The last revision replaced the ground motion attenuation models used in the Reference 233 model with the ground motion attenuation models developed in Reference 350 and the aleatory variability models developed by Reference 362. Subsection 2.5.2.4.4.3 summarizes the changes in ground motion models.

2.5.2.4.4.1 New Madrid Repeated Large Magnitude Earthquake Source

Characterization of the New Madrid source zone follows the model presented in the Clinton Early Site Permit (ESP) application (Reference 294), with one exception. For the New Madrid model recurrence rate calculation, the Clinton model used a time period of interest of 60 years whereas the Bellefonte model uses a time period of interest of 50 years. Both models assume 40-year plant lifetimes; however, the Bellefonte plant (Units 3 and 4) is expected to begin operation 10 years earlier than the Clinton plant. Thus, the time period of interest is 10 years shorter for Bellefonte relative to Clinton.

This discussion includes relevant new research published since the Clinton ESP was prepared. This new research does not change the Clinton characterization of the New Madrid seismic source.

Forte et al. (Reference 363) provide a new tectonic model for localizing strain in the new Madrid region involving descent of the ancient Farallon plate into the mantle. This new model helps explain large magnitude earthquakes in the New Madrid region, but does not provide additional information on the location, recurrence, or size of these earthquakes.

Recent research uses high precision GPS measurements to measure crustal motion within the New Madrid seismic zone. There is uncertainty as to the significance of data gathered to date (eg. References 364 and 365). However, the precision of velocity measurements is expected to increase as further measurements are made, such that these measurements eventually may be used to help delineate faults and determine present-day strain rates throughout the New Madrid seismic zone.

The principal seismic activity within the upper Mississippi embayment is interior to the Reelfoot rift along the NMSZ. Recent seismologic, geologic, and geophysical studies have associated faults within the NMSZ with large magnitude historical earthquakes that occurred during 1811-1812. Paleoliquefaction studies provide evidence that large magnitude earthquakes have occurred on these faults more frequently than the seismicity rates specified in the EPRI source characterizations. Figure 2.5-262 shows the locations of these sources relative to the BLN site.

The EPRI-SOG source characterizations, as they stand, adequately address the uncertainty related to location, magnitude, and frequency of earthquakes that may occur on other potential seismic sources in the region of the NMSZ, such as recently identified active faults along the northern and southern rift margins. Updating the EPRI-SOG seismic source evaluations for this study, therefore, focuses on the characterization of more frequent large magnitude events along the central fault system. The key source parameters are discussed in the following sections. The logic tree used to represent the uncertainty in the seismic source characterization model for the NMSZ central fault system is shown in Figure 2.5-263.

2.5.2.4.4.1.1 NMSZ Central Faults Source Geometry

Three fault sources are included in the updated characterization of the central fault system of the NMSZ: (1) the New Madrid South (NS) fault; (2) the New Madrid North (NN) fault; and (3) the Reelfoot fault (RF). The first three levels of the logic tree for these sources address the uncertainty in the research community regarding the location and extent of the causative faults that ruptured during the 1811-1812 earthquake sequence. This uncertainty is represented by alternative geometries for the NN, NS, and RF faults. These alternative geometries affect the distance from earthquake ruptures on these fault sources to the BLN site.

The locations of the faults that make up the New Madrid central fault system sources are shown in Figure 2.5-262 (inset A). For the New Madrid South fault (NS) source, two alternatives are considered, as described by Johnston and Schweig (Reference 366): (1) the BA/BL (BA/Bootheel lineament); and (2) the BA/ BFZ (BA/Blytheville fault zone). Although modern seismicity is occurring primarily along the BFZ, Johnston and Schweig (Reference 366) present arguments suggesting that the BA/BL is the most likely location for the main NM1 (D1) event and that major NM1 (D1) aftershocks occurred on the BFZ (the northeast extension of the Cottonwood Grove fault). Therefore, slightly greater weight is given to BA/BL [0.6] (total length of 132 kilometers [80 mi.]) versus BA/BFZ [0.4] (total length of 115 km [69 mi.]).

Recent work by Guccione et al. (Reference 367) suggests that the Bootheel lineament is a Holocene-active fault with primarily right lateral displacement. Surficial mapping and corehole transects reveal a Holocene paleochannel (2.4 ka) displaced dextrally at least 13 m across the lineament and a Pleistocene fluvial sand (10.2 ka) displaced vertically about 3 m. These observations, along with documentation of liquefaction features along the Bootheel lineament and observation in cores of juxtaposed sediment types across the lineament, leads to the conclusion that the Bootheel lineament is an active fault that kinematically links the New Madrid North and South faults.

Two alternative total lengths are considered for the NN source. The first, which is given the highest weight [0.7], allows for rupture of the 60-km (36-mi.) fault segment (NN, Figure 2.5-262) as defined by Johnston and Schweig (Reference 366). Cramer (Reference 368) uses a similar value 59 km (35.4 mi.) as the length of his northeast arm. Concentrated seismicity defines the segment as ~40 km (24 mi.) long. Johnston (Reference 297), in modeling the source fault for the NM2 (J1) earthquake, extends the fault to the epicentral region of the 1895 Charleston, Missouri, earthquake (6.0-6.6), for a total length of 65 km (39 mi.). An alternative total length of 97 km (58 mi.) allows for the fault to extend north to include less well-defined seismicity trends noted by Wheeler (Reference 262). Wheeler et al. (Reference 369) and other researchers argue for a structural northern boundary to the rift in this region. The New Madrid northern extension (NNE, Figure 2.5-262) is not as well defined by seismicity as is the NN segment. Also, the recurrence interval of large magnitude earthquakes in the northern Mississippi embayment appears significantly longer than the recurrence interval for NMSZ earthquakes based on

paleoliquefaction studies. Van Arsdale and Johnston (Reference 370) cite as evidence of a long recurrence interval (on the order of tens of thousands of years) the sparse seismicity, the lack of Holocene fault offsets in the Fluorspar Area fault complex along trend to the north, the presence of only minor Quaternary faulting, and the lack of discernable offset of the margins of Sikeston Ridge where it meets the NN. Given these observations, the longer (97 km [58 mi.]) fault length that includes the NN and NNE is given less weight [0.3].

Johnston and Schweig (Reference 366) conclude from historical accounts that the NM3 (F1) event occurred on the RF (Figure 2.5-264). Johnston and Schweig (Reference 366) identify three possible segments of the RF, a central 32-km (20-mi.)-long reverse fault defined by the RF scarp between the two northeasttrending strike-slip faults, a 35-km (22 mi.) -long segment (RS) that extends to the southeast, and a 40-km-long (24 mi.) segment west of the NN (Figure 2.5-264). Seismicity and geomorphic data indicate that the southeast segment is slightly shorter (25 to 28 km [16 to 17 mi.]) than indicated by (References 366, 371, and 372). Cramer (Reference 368) uses a total length of 60 kilometers for the RF. The alternative fault rupture scenarios of Johnston and Schweig (Reference 366) include rupture of a 40-km-long (24 mi.) northwest fault segment (Figure 2.5-264). Cramer (Reference 368) assigns a length of 33 km (21 mi.) to this segment, which he refers to as the west arm. Mueller and Pujol (Reference 372) note that this westerly arm is imaged as a vertical fault that terminates the Reelfoot thrust. They interpret the westerly arm as a left-lateral strike-slip fault kinematically linked to the Reelfoot thrust. Bakun and Hopper (Reference 338) suggest a preferred epicenter location at the northern end of the RS segment. Hough and Martin (Reference 373) show a slightly different geometry for the northwestern portion of the fault and do not interpret the historical 1811-1812 earthquake ruptures to have extended to the rift margin on the southeast (Figure 2.5-265). Two alternative fault geometries are included in this study: (1) the RF fault includes the NW, RF, and RS segments as defined in Cramer (Reference 368) and (2) a shorter RF that extends from the intersection with the NN fault and extends to the southeastern end of the RF as shown by Hough and Martin (Reference 373) (Figure 2.5-265). The longer length is judged to be more consistent with displacements and magnitudes inferred for the NM3 event, and thus is given higher weight in the model.

2.5.2.4.4.1.2 NMSZ Central Faults Maximum Earthquake Magnitude

The next level of the logic tree addresses the maximum magnitude for earthquakes on the three New Madrid fault sources. As discussed previously in section (a), specific faults and seismicity lineaments have been proposed as the sources of the 1811-1812 and previous earthquakes. In addition, researchers have suggested that the sizes of prehistoric earthquakes associated with these sources are similar to the 1811-1812 earthquakes (e.g., Reference 374). The identification of fault sources and repeated large earthquakes of similar size is suggestive of the behavior of crustal faults in more active regions and many recent studies (e.g., References 269, 348, 349 and 351) have used the concept of “characteristic” earthquakes to characterize the behavior of

the New Madrid seismic source. The characteristic earthquake concept is that a seismic source generates repeated large earthquakes of similar size at a frequency that is greater than obtained by extrapolating a Gutenberg-Richter recurrence relationship fit to the observed seismicity rate for smaller-magnitude earthquakes, as illustrated in Figure 2.5-249. These characteristic earthquakes represent the largest earthquakes produced by the source, and as such represent the maximum magnitude event. Using the concept of characteristic earthquakes, seismic source characterizations of the New Madrid seismic source zone typically consider the 1811-1812 earthquakes to represent the maximum earthquake for this source. Table 2.5-213 summarizes recent estimates of the magnitude of the New Madrid 1811-1812 mainshocks.

Bakun and Hopper (Reference 338) provide preferred estimates of the locations and moment magnitudes and their uncertainties for the three largest events in the 1811-1812 sequence near New Madrid. Their preferred intensity magnitude M_I , which is their preferred estimate of M , is 7.6 (6.8 to 7.9 at the 95 percent confidence interval) for the December 16, 1811, Event (NM1), 7.5 (6.8 to 7.8 at the 95 percent confidence interval) for the January 23, 1812, Event (NM2), and 7.8 (7.0 to 8.1 at the 95 percent confidence interval) for the February 7, 1812, Event (NM3). The intensity magnitude M_I is the mean of the intensity magnitudes estimated from individual MMI assignments. In their analysis, Bakun and Hopper (Reference 338) consider two alternative eastern North America (ENA) intensity attenuation models, which they refer to as models 1 and 3. As indicated in Table 2.5-213, these two models give significantly different results for larger magnitude earthquakes. Bakun and Hopper (Reference 338) state that because these models are empirical relations based almost exclusively on $M < 6$ calibration events “There is no way to confidently predict which relation better represents the MMI-distance data for $M > 7$ earthquakes in ENA” (p. 66, Reference 338). They present arguments supporting their preference for model 3, but do not discount the results based on model 1.

Dr. Susan Hough (Reference 375) believes that there are insufficient data regarding the calibration of ENA earthquakes larger than $M > 7$ to rely strictly on ENA models as was done in Bakun and Hopper (Reference 338). She offers arguments to support $M < 7.6$ (the size of the 2003 Bhuj earthquake) as a reasonable upper bound for the largest of the earthquakes in the 1811-1812 New Madrid earthquake sequence, which is more consistent with the estimates cited in Hough et al. (Reference 376) and Mueller et al. (Reference 377).

Mueller et al. (Reference 377) use instrumentally recorded locations of recent earthquakes (assumed by Mueller et al. to be aftershocks of the 1811-1812 sequence) and models of elastic stress change to develop a kinematically consistent rupture scenario for the mainshock earthquakes of the 1811-1812 New Madrid sequence. In general, the estimated magnitudes for NM1 and NM3 used in their analysis ($M = 7.3$ and $M = 7.5$, respectively) are consistent with those previously published by Hough et al. (Reference 376). Their results suggest that the mainshock Events NM1 and NM3 occurred on two contiguous faults, the strike-slip Cottonwood Grove fault and the Reelfoot thrust fault, respectively. The locations of the NM1 and NM3 Events

on the Cottonwood Grove and RFs, respectively, are relatively well constrained. In contrast to the earlier Hough et al. (Reference 376) study that located the NM2 earthquake on the NN, they suggest a more northerly location for the NM2 Event, possibly as much as 200 km (124 mi.) to the north in the Wabash Valley of southern Indiana and Illinois. Hough et al. (Reference 378) also infer a similar more northerly location. Using Bakun and Wentworth's (Reference 379) method, Mueller et al. (Reference 377) obtain an optimal location for the NM2 mainshock at 88.43°W, 36.95°N and a magnitude of **M** 6.8. They note that the location is not well constrained and could be fit almost as well by locations up to 100 km (62 mi.) northwest or northeast of the optimal location. Mueller et al. (Reference 377) conclude that the three events on the contiguous faults increased stress near fault intersections and end points in areas where present-day microearthquakes have been interpreted as evidence of primary mainshock rupture. They note that their interpretation is consistent with established magnitude/fault area results, and do not require exceptionally large fault areas or stress drop values for the New Madrid mainshocks.

With respect to the location of the NM2 Event, Bakun and Hopper (Reference 338) also discuss the paucity of MMI assignments available for this earthquake to the west of the NMSZ and the resulting uncertainty in its location. They note that the two MMI sites closest to the NMSZ provide nearly all of the control on the location of this event and that, based on these two sites, a location northeast of their preferred site would be indicated. However, they conclude that the lack of 1811-1812 liquefaction observations in western Kentucky, southern Illinois, and southern Indiana preclude an NM2 location in those areas. Bakun and Hopper (Reference 338) follow Johnston and Schweig (Reference 366) in selecting a preferred location on the NN. Dr. Steve Obermeier confirmed that liquefaction features in the Wabash Valley region that would support the more northerly location preferred by Mueller et al. (Reference 377) are absent (Reference 380). He noted that he had looked specifically in the area cited in the Yearby Land account that was cited by Mueller et al. (Reference 377) and observed evidence for only small sand blows and dune sands, but did not see features of the size and origin described in that account.

The review of these new publications indicates that there still remain uncertainty and differing views within the research community regarding the size and location of the 1811-1812 earthquakes. In addition, Dr. Arch Johnston (Reference 381) indicates that the estimates of Johnston (Reference 297) are likely to be high by about 0.2 to 0.3 magnitude units. Based on this review of these articles and the communications with Drs. Bakun, Hough, and Johnston, the maximum magnitude for the New Madrid central fault system faults was defined as follows.

- Equal weight (one-third) is to be given to estimates based on Bakun and Hopper (Reference 338) and Hough et al. (Reference 376)/Mueller et al. (Reference 377), and the Johnston (Reference 381) revisions to Johnston (Reference 297)
- Results from both intensity attenuation relations (models 1 and 3) in the Bakun and Hopper (Reference 338) estimate are used. Based on Bakun and Hopper's preference for model 3, weights are assigned of 0.75 to model 3 and 0.25 to model 1

- In the case of the Hough et al. (Reference 376)/Mueller et al. (Reference 377) estimates and Hough (Reference 375) estimates, equal weight is assigned to the range of preferred values given for each earthquake.

The resulting characteristic magnitude distribution for each of the three faults is given in Table 2.5-214. Rupture sets 1 and 2 correspond to the revised Johnston (Reference 297) estimates, rupture sets 3 and 4 correspond to the Bakun and Hopper (Reference 338) estimates, and rupture sets 5 and 6 correspond to the Hough et al. (Reference 376) estimates.

As discussed in the following section, the present interpretation of the paleoearthquake data is that the two prehistoric earthquake ruptures that occurred before the 1811-1812 sequence also consisted of multiple, large magnitude earthquakes. Therefore, for this assessment, the event is considered to be rupture of multiple (two to three) of the fault sources shown in Figure 2.5-262. Furthermore, the arguments for the high versus low magnitude assessments for the individual faults are considered to be highly correlated. Therefore, six alternative sets of ruptures were produced from the distributions developed previously for each fault, as shown in the logic tree in Figure 2.5-263 and given in Table 2.5-214.

The magnitudes listed in Table 2.5-214 are considered to represent the size of the expected maximum earthquake rupture for each fault within the NMSZ. Following the development of the characteristic earthquake recurrence model by Youngs and Coppersmith (Reference 357), as modified by Youngs et al. (Reference 382), the size of the next characteristic earthquake is assumed to vary randomly about the expected value following a uniform distribution over the range of $\pm\frac{1}{4}$ magnitude units. This range represents the aleatory variability in the size of individual characteristic earthquakes. For example, given that the expected magnitude for the characteristic earthquake on the NS fault source is **M** 7.8, the magnitude for the next characteristic earthquake is uniformly distributed between **M** 7.55 and **M** 8.05.

2.5.2.4.4.1.3 NMSZ Central Faults Earthquake Recurrence

The best constraints on recurrence of repeated large magnitude NMSZ events result from paleoliquefaction studies throughout the New Madrid region and paleoseismic investigations of the RF scarp and associated fold. Based on studies of hundreds of earthquake-induced paleoliquefaction features at more than 250 sites, Tuttle et al. (Reference 374) conclude that: (1) the fault system responsible for the New Madrid seismicity generated temporally clustered, very large earthquakes in AD 900 \pm 100 and AD 1450 \pm 150 years as well as in 1811-1812; (2) given uncertainties in dating liquefaction features, the time between the past three events may be as short as 200 years or as long as 800 years, with an average of 500 years; and (3) prehistoric sand blows probably are compound structures, resulting from multiple earthquakes closely clustered in time (i.e., earthquake sequences).

A recent paleoliquefaction study in the northern part of the New Madrid seismic zone supports these conclusions (Reference 352). Six episodes of earthquake-induced liquefaction are associated with soil horizons containing artifacts and datable organic material. The oldest four

episodes of liquefaction occurred around 2350 B. C (4350 ybp) +200 years and are interpreted to represent a cluster of earthquakes similar in size to the 1811-1812 New Madrid earthquakes. Two later episodes of liquefaction are documented to have occurred in A.D 300 (1700 ybp) +200 years, and A.D 1670. A New Madrid-type earthquake in 300 A.D. would be support and average recurrence time of 500 years.

The full paleoseismic record of the New Madrid seismic zone is reviewed by Guccione (Reference 383). The record includes evidence from paleoliquefaction, sediment rupture and deformation, fluvial response, and biotic response, Interdisciplinary approaches to paleoseismology have provided a well constrained catalog of Late Holocene earthquake events. Five well-dated large seismic events have occurred during the Late Holocene, and several less-well-dated events are documented during the Early and Middle Holocene.

Periodic channel perturbations in the Mississippi River across the Reelfoot fault are documented by Holbrook et al. (Reference 384), and assumed to correlate with seismic events that caused vertical displacements across the fault. Analysis of sequentially abandoned meander bends suggests that channel straightening events occurred upstream of the Reelfoot fault in the previously known A.D 900, event, documented by Kelson et al. (Reference 385). Another river-straightening event occurred between 4244 ± 269 ybp and 3620 ± 220 ybp. This research contributes evidence for activity on the Reelfoot fault in the middle Holocene.

Cramer (Reference 368) obtained a 498-year mean (440-year median) recurrence interval for New Madrid characteristic earthquakes based on a Monte Carlo sampling of 1,000 recurrence intervals using the Tuttle and Schweig (Reference 391) uncertainties as a range of permissible dates (\pm two standard deviations) for the two most recent prehistoric earthquakes (i.e., AD 900 \pm 100 and AD 1450 \pm 135). Assuming a lognormal distribution with a coefficient of variation of 0.5 for inter-arrival time, Cramer (Reference 368) obtained a 68 percent confidence interval for the mean recurrence interval of 267 to 725 years, and a 95 percent confidence interval of 162 to 1196 years (ranges for one and two standard deviations, respectively).

Exelon (Reference 294, Attachment 2 to Appendix B) presents a detailed assessment of the timing constraints on prehistoric New Madrid earthquakes and the development of occurrence rates for repeats of 1811-1812 earthquake sequence. The uncertainties in the ages of individual samples were used to constrain the timing of individual events. A Monte Carlo sample of 10,000 sets of time intervals between events was generated using these data. Two recurrence models were used to represent the occurrence of earthquake sequences, the commonly used Poisson (memoryless) model and a renewal model (one-step memory). The uncertainty in fitting these models to a sample of limited size (two closed time intervals, between 900 AD and 1450 AD and between 1450 AD and 1811-1812, and one open interval post 1812) together with the simulated distributions of time intervals provided uncertainty distributions on the recurrence rates for New Madrid sequences. For the renewal model, Exelon (Reference 294) used a lognormal distribution to represent the time between earthquakes. Exelon (Reference 356) repeated the

analysis of the simulated time intervals between earthquake sequences using the Brownian Passage Time (BPT) model developed by Ellsworth et al. (Reference 387) and Matthews et al. (Reference 388) to represent the distribution of the time between earthquake sequences in the renewal model. Ellsworth et al. (Reference 387) and Matthews et al. (Reference 388) propose that the BPT model is more representative of the physical process of strain buildup and release on a seismic source than the other distribution forms that have been used for renewal models (e.g., the lognormal). Based on these arguments, the BPT model was used by the Working Group (Reference 389) to assess the probabilities of large earthquakes in the San Francisco Bay area. Figure 2.5-266 shows the uncertainty distributions for the mean repeat time between New Madrid earthquake sequences obtained by Exelon (Reference 356). Application of the BPT model requires estimation of the aperiodicity coefficient α that defines the variability in the timing of individual events. Because of the very limited sample size, Exelon (Reference 356) did not estimate α from the simulated data. Instead, they utilized the distribution for α developed by the Working Group (Reference 389) of 0.3 (wt 0.2), 0.5 (wt 0.5), and 0.7 (wt 0.3). These alternative values were incorporated into the uncertainty model for the New Madrid repeating earthquake source (Figure 2.5-263).

Following the process used by Exelon (References 294 and 356), the occurrence rates for New Madrid large magnitude earthquake sequences were estimated using the distributions for mean repeat time shown in Figure 2.5-266. For the Poisson model, the occurrence rate is just the inverse of the mean repeat time. For the BPT-renewal model, an equivalent Poisson rate is obtained, allowing the exceedance rate from the New Madrid earthquake sequence to be added to the exceedance rate from all other sources. The equivalent Poisson rate, $\lambda_{renewal}$, is given by the expression:

$$\lambda_{renewal} = -\ln[1 - P_{renewal}(\text{event in time } t_0 \text{ to } t_0 + \Delta t)] / \Delta t \quad (2.5.2-9)$$

where t_0 is the present time measured from the date of the most recent event, Δt is the time period of interest, and $P_{renewal}(t)$ is the probability of the event occurring in the time interval Δt . The time period of interest, Δt , was taken to be 50 years. This is a somewhat long for the typical life span of a nuclear power plant, but longer values of Δt produce larger values of the average rate. The renewal recurrence model, $P_{renewal}(t)$ is given by the expression:

$$P_{renewal}(\text{event in time } t_0 \text{ to } t_0 + \Delta t) = \frac{F(t_0 + \Delta t) - F(t_0)}{1 - F(t_0)} \quad (2.5.2-10)$$

where $F(t)$ is the cumulative distribution for time between events.

Equation (2.5.2-10) gives the probability of a single event in time Δt while the equivalent Poisson rate (Equation 2.5.2-9) is based on the probability of one or more events. However, the probability of two or more in the renewal model case is negligible.

For the BPT model, $F()$ is given by:

$$F(t) = \Phi[u_1(t)] + e^{2/\alpha^2} \Phi[-u_2(t)]$$

$$u_1(t) = (\sqrt{t/\mu} - \sqrt{\mu/t})/\alpha$$

$$u_2(t) = (\sqrt{t/\mu} + \sqrt{\mu/t})/\alpha$$

$$f(t) = \left(\frac{\mu}{2\pi\alpha^2 t^3}\right)^{1/2} \exp\left(-\frac{(t-\mu)^2}{2\mu\alpha^2 t}\right) \quad (2.5.2-11)$$

where μ is the mean inter-arrival time (repeat time), α is the aperiodicity coefficient, and $\Phi()$ is the standard normal cumulative probability function.

The uncertainty distributions for mean repeat time shown in Figure 2.5-266 were represented in the seismic hazard model by a five-point discrete approximation to a continuous distribution developed by Miller and Rice (Reference 390). Table 2.5- 215 lists the discrete distributions for mean repeat time and the equivalent Poisson rates. The Poisson and renewal recurrence models are given equal weight (Figure 2.5-263). The renewal model is considered more appropriate on a physical basis for the behavior of characteristic earthquakes on active faults. The Working Group (Reference 389) applied weights of 0.7 and 0.6 to non-Poissonian behavior for the San Andreas and Hayward faults, respectively. For other, less active sources, they assigned a weight of 0.5 or less to non-Poissonian behavior. While the New Madrid faults are not plate boundary faults, they exhibit behavior that is similar to that expected for an active plate boundary fault. Equal weights represent maximum uncertainty as to which is the more appropriate model.

The paleoliquefaction data gathered in the New Madrid region indicate that the prehistoric earthquakes have occurred in sequences closely spaced in time relative to the time period between sequences, similar to the 1811-1812 sequence. Figure 2.5-267, taken from Tuttle et al. (Reference 374), shows the estimated earthquake sizes and event locations for the 1811-1812 sequence and the two previous sequences. These data indicate that the RF has ruptured in all three sequences, but the NN and NS sources may have produced earthquakes on the order of one magnitude unit smaller than the 1811-1812 earthquakes in previous sequences. Recent discussions with Dr. Tuttle (Reference 386) indicate that she considers that the difference between the size of the 1811-1812 earthquakes and those of the 900 and 1450 sequences are likely to be smaller than what was portrayed in Figure 6 of Tuttle et al. (Reference 374). As a result, Exelon (Reference 356) revised the model of Exelon (Reference 294) for New Madrid sequences to consist of two alternative models of rupture or earthquake sequences. In Model A, all ruptures are similar in size to the 1811-1812 earthquakes. In Model B one-third of the

sequences are the same as Model A, one-third of sequences contain a smaller rupture of the NN, and one-third of sequences contain a smaller rupture of the NS. The difference in magnitude from the 1811-1812 ruptures was set to be no more than one-half magnitude unit, and no ruptures are allowed to be less than **M** 7. All three earthquakes were included in the hazard calculation in all rupture sequences. Model A (always full ruptures) is given a weight of two-thirds and Model B a weight of one-third, based on Dr. Tuttle's expression of the difficulties in estimating the size of the pre 1811-1812 ruptures and her judgment that the difference between the rupture sizes was likely smaller than proposed in Tuttle et al. (Reference 374).

The computation of the hazard from the New Madrid earthquake sequence uses the formulation outlined in Toro and Silva (Reference 351). The frequency of exceedance, $v(z)$, from the earthquake sequence is given by the expression:

$$v(z)_{sequence} = \lambda_{sequence} \left[1 - \prod_i \{1 - P_i(Z > z)\} \right] \quad (2.5.2-12)$$

where $\lambda_{sequence}$ is the equivalent annual frequency of event clusters and $P_i(Z > z)$ is the probability that earthquake i in the sequence produces ground motions in excess of level z .

2.5.7 REFERENCES

- 203. Electric Power Research Institute, Seismicity Owners Group, *Seismic Hazard Methodology for the Central and Eastern United States*, Technical Report NP-4726-A, Vols 1-10, 1988.
- 213. Hatcher, R. D., Jr., "Tectonic Synthesis of the U.S. Appalachians," in Hatcher, R.D., Jr., W. A. Thomas, and G. W. Viele, eds., *The Appalachian-Ouachita Orogen in the United States. Boulder, Colorado: Geological Society of America, the Geology of North America*, Vol F-2, Chapter 14, pp. 511-535, 1989.
- 233. Electric Power Research Institute, *Probabilistic Seismic Hazard Evaluations at Nuclear Power Plant Sites in the Central and Eastern United States*, Technical Report NP-6395-D, 1989.
- 262. Wheeler, R. L., "Boundary Separating the Seismically Active Reelfoot Rift from the Sparsely Seismic Rough Creek Graben, Kentucky, and Illinois." *Seismological Research Letters*. Vol. 68. pp. 586-598, 1997.
- 269. Geomatrix Consultants, Inc. , *Dam Safety Seismic Hazard Assessment*, Report prepared for the Tennessee Valley Authority, Vols 1 and 2, September 2004.
- 294. Exelon Generation Company, LLC, Site Safety Analysis Report, Clinton Early Site Permit Application, Revision 4, Docket No 05200007, April 14, 2006.

297. Johnston, A. C., "Seismic Moment Assessment of Earthquakes in Stable Continental Regions—III, New Madrid 1811-1812, Charleston 1886, and Lisbon 1755," *Geophysical Journal International*, Vol 126, No 3, pp. 314-344, 1996.
338. Veneziano, D., and J. Van Dyck, *Analysis of Earthquake Catalogs for Incompleteness and Recurrence Rates: Seismic Hazard Methodology for Nuclear Facilities in the Eastern United States*. EPRI Research Project N. P101-29. EPRI/SOG Draft 85-1. Vol. 2, Appendix A. April 30, 1985.
348. Frankel, A. D., M. D. Petersen, C. S. Mueller, K. M. Haller, R. L. Wheeler, E. V. Leyendecker, R. L. Wesson, S. C. Harmsen, C. H. Cramer, D. M. Perkins, and K. S. Rukstales, *Documentation for the 2002 Update of the National Seismic Hazard Maps*, U.S. Geological Survey Open-File Report 02-420, 33 pp., 2002.
349. Frankel, A., C. Mueller, T. Barnhard, D. Perkins, E.V. Leyendecker, N. Dickman, S. Hanson, and M. Hopper, *National Seismic-Hazard Maps; Documentation*, U.S. Geological Survey Open-File Report 96-532, 110 pp., 1996.
350. Electric Power Research Institute, *CEUS Ground Motion Project Final Report*, Technical Report 1009684, 2004.
351. Toro, G. R., and W. J. Silva, *Scenario Earthquakes for Saint Louis, MO, and Memphis, TN, and Seismic Hazard Maps for the Central United States Region Including the Effect of Site Conditions*. Final Technical Report prepared by Risk Engineering, Inc., Boulder, Colorado, under U.S. Geological Survey External Grant No. 1434-HQ-97-02981. January 10, 2001.
352. Tuttle, M. P., E. S. Schweig III, J. Campbell, P. M. Thomas, J. D. Sims, and R. H. Lafferty III, "Evidence for New Madrid Earthquakes in AD 300 and 2350 B.C." *Seismological Research Letters*. Vol. 76. pp. 489-501, 2005.
356. Exelon Generation Company, LLC, Response to Request for Additional Information Letter No 7, Early Site Application for Clinton Site, October 11, 2004.
357. Youngs, R. R., and K. J. Coppersmith, "Implications of Fault Slip Rates and Earthquake Recurrence Models to Probabilistic Hazard Estimates." *Bulletin of the Seismological Society of America*. Vol. 75. pp. 939-964, 1985.
362. Abrahamson, N.A., and J. Bommer, *Program on Technology Innovation: Truncation of the Lognormal Distribution and Value of the Standard Deviation for ground Motion Models in the Central and Eastern United States*, Electric Power Research Institute, Report 1014381, 2006.

363. Forte, A. M., R. Moucha; J. X. Mitrovica, N. A. Simmons and S. P. Grand: Descent of the ancient Farallon slab drives localized mantle flow below the New Madrid seismic zone: *Geophysical Research Letters* 10.1029/2006GL027895, 2007
364. Tuttle, Martitia P., New Madrid in motion: *Nature*, v. 435, pp. 1037-1039, 2005.
365. Stein, Seth, New Madrid GPS: Much Ado About Nothing?: *EOS, Transactions American Geophysical Union*, v. 88, no. 5, p. 59, 2007
366. Johnston, A. C., and E. S. Schweig, "The Enigma of the New Madrid Earthquakes of 1811-1812." *Annual Review, Earth Planet. Science*. Vol. 24. pp. 339-384, 1996.
367. Guccione, Margaret J., Marple, R., and Autin, W.J., Evidence for Holocene displacements on the Bootheel fault (lineament) in southeastern Missouri: Seismotectonic implications for the new Madrid region: *Geological Society of America Bulletin*, v. 117, no 3/4, p. 319-333, 2005.
368. Cramer, C. H., "A Seismic Hazard Uncertainty Analysis for the New Madrid Seismic Zone," *Engineering Geology*, Vol 62, pp. 251-266, 2001.
369. Wheeler, R. L., S. Rhea, S. F. Diehl, J. A. Drahovzal, G. W. Bear, and M. L. Sargent, *Seismotectonic Map Showing Faults, Igneous Rocks, and Geophysical and Neotectonic Features in the Vicinity of the Lower Wabash Valley, Illinois, Indiana, and Kentucky*. U.S. Geological Survey Geologic Investigations Series I-2583-D, 1997.
370. Van Arsdale, R. B., and A. Johnston, "Geological and Seismological Setting of the New Madrid Seismic Zone and the Wabash Valley Seismic Zone." Appendix A of Risk Engineering, Inc. 1999. *Updated Probabilistic Seismic Hazard Analysis for the Paducah Gaseous Diffusion Plant, Paducah, Kentucky*. Report prepared for Lockheed Martin Utility Systems, Inc., U.S. Nuclear Regulatory Commission Docket 07007001. April 26, 1999.
371. Van Arsdale, R. B., R. T. Cox, A. C. Johnston, W. J. Stephenson, and J. K. Odum, "Southeastern Extension of the Reelfoot Fault." *Seismological Research Letters*. Vol. 70. No. 3. pp. 348-359, 1999.
372. Mueller, K. and J. Pujol, "Three-Dimensional Geometry of the Reelfoot Blind Thrust: Implications for Moment Release and Earthquake Magnitude in the New Madrid Seismic Zone." *Bulletin of the Seismological Society of America*. Vol. 91. pp. 1563-1573, 2001.
373. Hough, S. E., and S. Martin, "Magnitude Estimates of Two Large Aftershocks of the 16 December 1811 New Madrid Earthquake," *Bulletin of the Seismological Society of America*, Vol 92, No 8, pp. 3259-3268, 2002.

374. Tuttle, M. P., E. S. Schweig, J. D. Sims, R. H. Lafferty, L. W. Wolf, and M. C. Haynes, "The Earthquake Potential of the New Madrid Seismic Zone." *Bulletin of the Seismological Society of America*. Vol. 92. No. 6. pp. 2080-2089, 2002.
375. Hough, Dr. Susan, U. S. Geological Survey, personal (electronic) communication, August 23, 2004.
376. Hough, S., J. G. Armbruster, L. Seeber, and J. F. Hough, "On the Modified Mercalli Intensities and Magnitudes of the 1811-1812 New Madrid, Central United States, Earthquakes." *Journal of Geophysical Research*. Vol. 105. No. B10. pp. 23,839-23,864, 2000.
377. Mueller, K., S. E. Hough, and R. Billham, "Analysing the 1811-1812 New Madrid Earthquakes with Recent Instrumentally Recorded Aftershocks." *Nature*. Vol. 429. pp. 284-288, 2004.
378. Hough, S. E., R. Bilham, K. Mueller, W. Stephenson, R. Williams, and J. Odum, "Wagon Loads of Sand Blows in White County, Illinois." *Seismological Research Letters*. Vol. 76. No. 3. pp. 373-386, 2005.
379. Bakun, W. H., and C. M. Wentworth, "Estimating Earthquake Location and Magnitude from Seismic Intensity Data," *Bulletin of the Seismological Society of America* 87:1502-1521, 1997.
380. Obermeier, S. F. U.S. Geological Survey, Emeritus, Reston, Virginia; EqLiq Consulting, personal (electronic) communication, August 24, 2004.
381. Johnston, A. C., CERL, University of Memphis, personal communication, August 31, 2004.
382. Youngs, R. R., F. H. Swan, and M. S. Power, "Use of Detailed Geologic Data in Regional PSHA: an Example from the Wasatch Front, Utah." In J.L. Von Thun, ed. *Earthquake Engineering and Soil Dynamics II—Recent Advances in Ground Motion Evaluation*. pp. 156-172, 1988.
383. Guccione, Margaret J., Late Pleistocene and Holocene paleoseismology of an intraplate seismic zone in a large alluvial valley, the New Madrid seismic zone, Central USA: *Tectonophysics*, v. 408, pp. 237-264, 2005.
384. Holbrook, J., Autin, W.J., Rittenour, T.M., Marshak, S., and Goble, R.J., Stratigraphic evidence for millennial-scale temporal clustering of earthquakes on a continental-interior fault: Holocene Mississippi River floodplain deposits, New Madrid seismic zone, USA: *Tectonophysics*, v. 420, pp. 431-454, 2006.

385. Kelson, K. I., G. D. Simpson, R. B. Van Arsdale, C. C. Haraden, and W. R. Lettis, "Multiple Late Holocene Earthquakes Along the Reelfoot Fault, Central New Madrid Seismic Zone." *Journal of Geophysical Research*. Vol. 101. No. B3. pp. 6151-6170, 1996.
386. Tuttle, M. P., M. Tuttle & Associates, personal communication, August 24, 2004.
387. Ellsworth, W. L., M. V. Matthews, R. M. Nadeau, S. P. Nishenko, P. A. Reasenber, and R. W. Simpson, "A Physically-based Earthquake Recurrence Model for Estimation of Long-Term Earthquake Probabilities," *Proceedings of the Workshop on Earthquake Recurrence: State of the Art and Directions for the Future*, Istituto Nazionale de Geofisica, Rome, Italy, February 22-25, 1999.
388. Matthews, M. V., W. L. Ellsworth, and P. A. Reasenber, "A Brownian Model for Recurrent Earthquakes," *Bulletin of the Seismological Society of America*. Vol 92, pp. 2233-2250, 2002.
389. Working Group on California Earthquake Probabilities, *Earthquake Probabilities in the San Francisco Bay Region: 2002-2031*. U.S. Geological Survey Open-File Report 03-214, 2003.
390. Miller, A. C., and T. R. Rice, "Discrete Approximations of Probability Distributions," *Management Science*, Vol 29, pp. 352-362, 1983.
391. Tuttle, M. P., and E. S. Schweig, "The Earthquake Potential of the New Madrid Seismic Zone." *American Geophysical Union, EOS Transactions*. Vol. 81. No. 19. p. S308, 2000.

TABLE 2.5.2-213 MAGNITUDE COMPARISONS FOR NEW MADRID 1811-1812 EARTHQUAKE SEQUENCE

Study	NM1	NM2	NM3
Johnston (1996) (Reference 213)	M 8.1 ± 0.3	M 7.8 ± 0.3	M 8.0 ± 0.3
Hough et. al. (2000) (Reference 376)	M 7.2 to 7.3	M ~7.0 ^(a) (located on the NN)	M 7.4 to 7.5
Mueller and Pujol (2001) (Reference 372)	-	-	M 7.2 to 7.4 (preferred M 7.2 to 7.3)
Bakun and Hopper (2004) (Reference 296)	M 7.6 (M 7.2 to 7.9) (preferred model 3)	M 7.5 (M 7.1 to 7.8) (preferred model 3)	M 7.8 (M 7.4 to 8.1) (preferred model 3)
	M 7.2 (M 6.8 to 7.9) (model 1)	M 7.2 (M 6.8 to 7.8) (model 1)	M 7.4 (M 7.0 to 8.1) (model 1)
Mueller et. al. (2004) (Reference 377)	M 7.3	M 6.8 (located within the Wabash Valley of southern Illinois/ southern Indiana)	M 7.5
	M 7.8 to 7.9	M 7.5 to 7.6	M 7.7 to 7.8
Johnston (2001) (Reference 381)	M 7.8 to 7.9	M 7.5 to 7.6	M 7.7 to 7.8

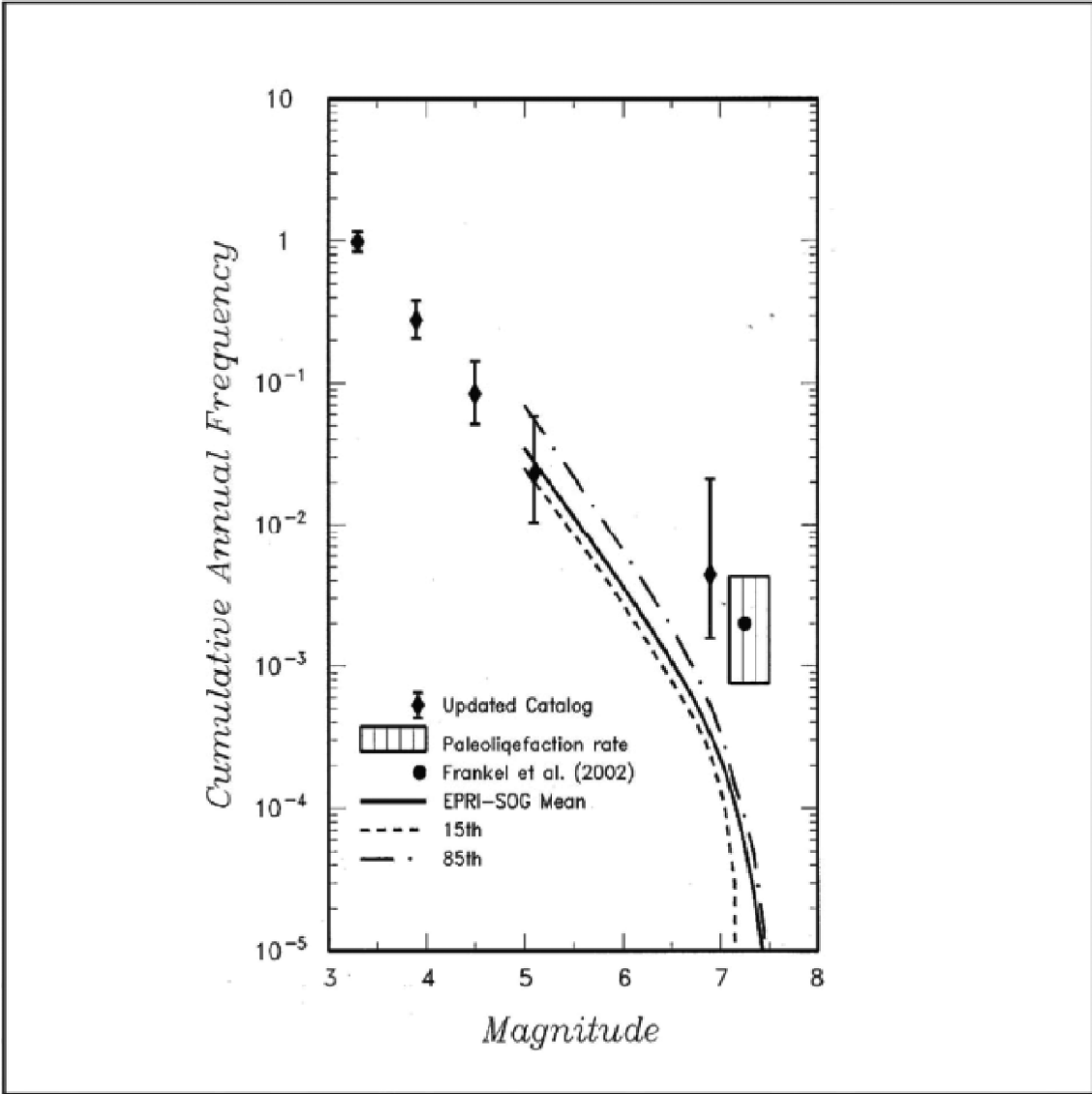
a) The estimated location and magnitude of this earthquake are revised in Mueller et. al. (2004) (Reference 377).

**TABLE 2.5.2-214 MAGNITUDE DISTRIBUTIONS FOR REPEATING LARGE-MAGNITUDE
 NEW MADRID EARTHQUAKES**

Earthquake Rupture Set	Magnitude for Individual Faults (moment magnitude [M])			Weight
	New Madrid South	Reelfoot Thrust	New Madrid North	
1	7.8	7.7	7.5	0.1667
2	7.9	7.8	7.6	0.1667
3	7.6	7.8	7.5	0.25
4	7.2	7.4	7.2	0.0833
5	7.2	7.4	7.0	0.1667
6	7.3	7.5	7.0	0.1667

TABLE 2.5.2-215 EARTHQUAKE FREQUENCIES FOR REPEATING LARGE-MAGNITUDE EARTHQUAKES (Sheet 1 of 7)

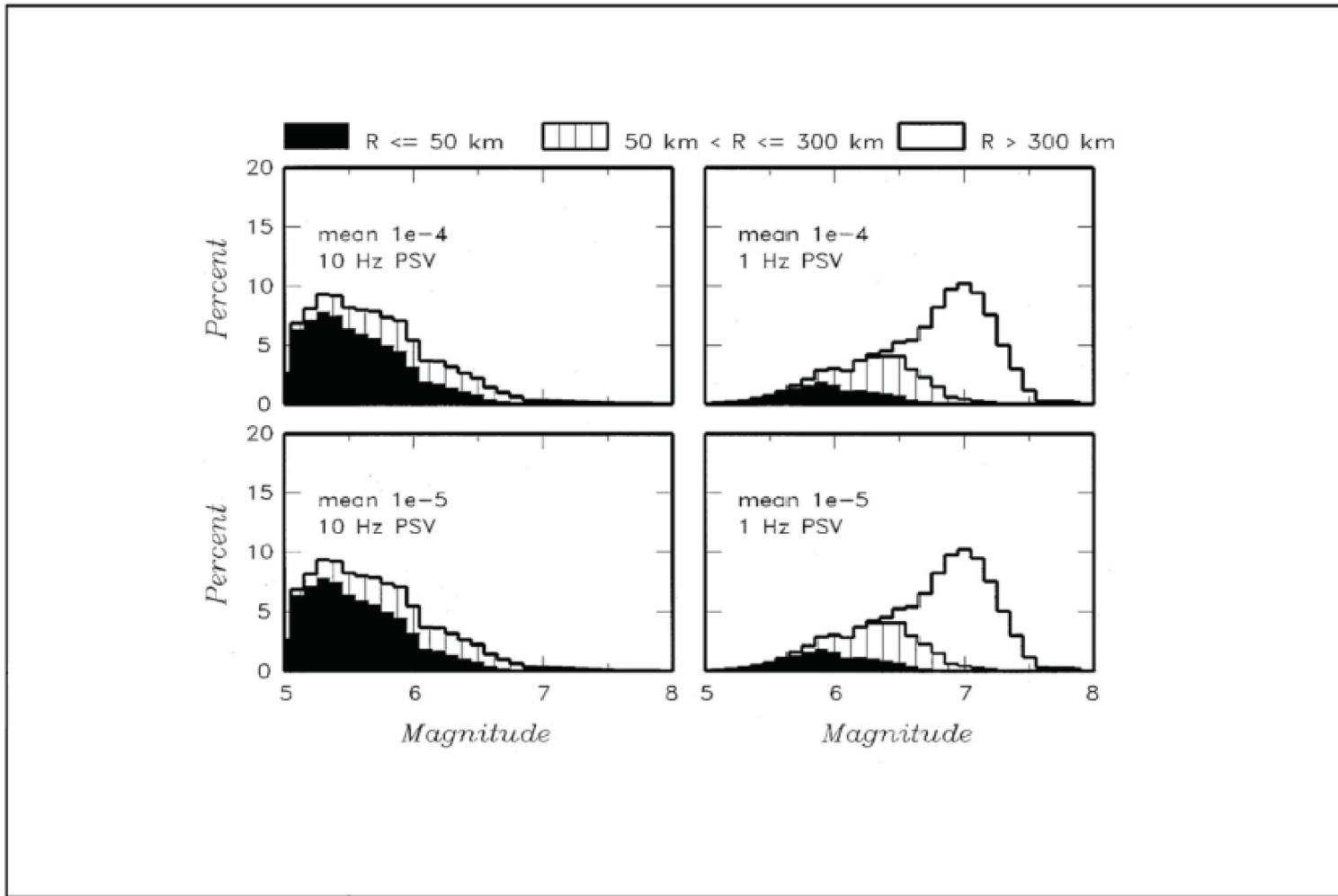
Recurrence Model	Weight	Mean Repeat Time (years)	Equivalent Annual Frequency
New Madrid Poisson	0.10108	160	6.26E-03
	0.24429	259	3.86E-03
	0.30926	407	2.46E-03
	0.24429	685	1.46E-03
	0.10108	1,515	6.60E-04
	0.10108	325	3.32E-03
New Madrid Renewal, $\alpha = 0.3$	0.24429	401	9.96E-04
	0.30926	475	2.67E-04
	0.24429	562	4.98E-05
	0.10108	695	3.22E-06
	0.10108	310	4.87E-03
New Madrid Renewal, $\alpha = 0.5$	0.24429	430	2.19E-03
	0.30926	559	8.81E-04
	0.24429	728	2.49E-04
	0.10108	1,008	2.72E-05
	0.10108	318	4.53E-03
New Madrid Renewal, $\alpha = 0.7$	0.24429	494	2.28E-03
	0.30926	701	1.03E-03
	0.24429	986	3.35E-04
	0.10108	1,484	4.30E-05



(Reference 348)

BLN COL 2.5-2

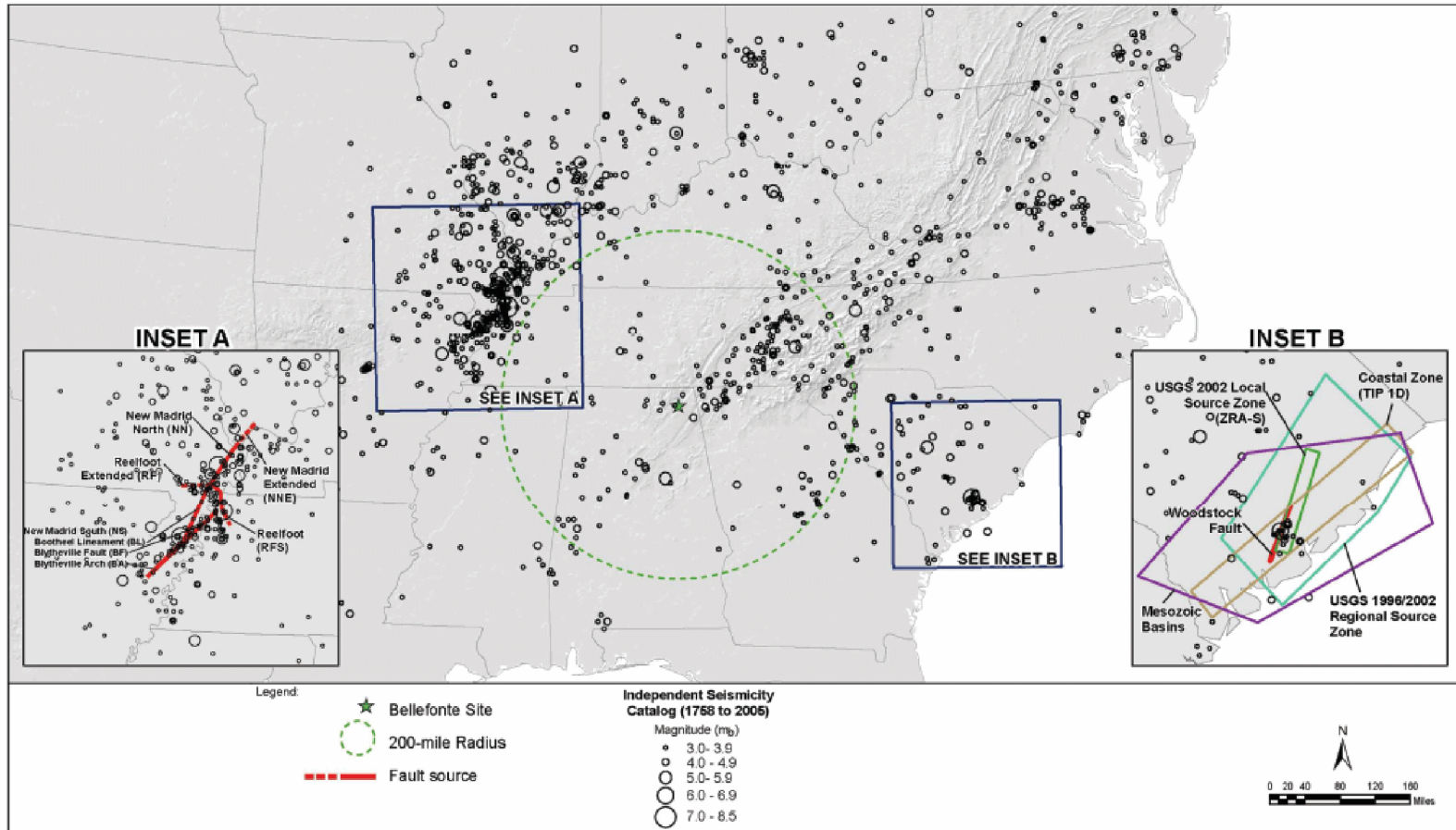
FIGURE 2.5-249
Earthquake Recurrence Rates for New Madrid Seismic Sources



(Reference 203)

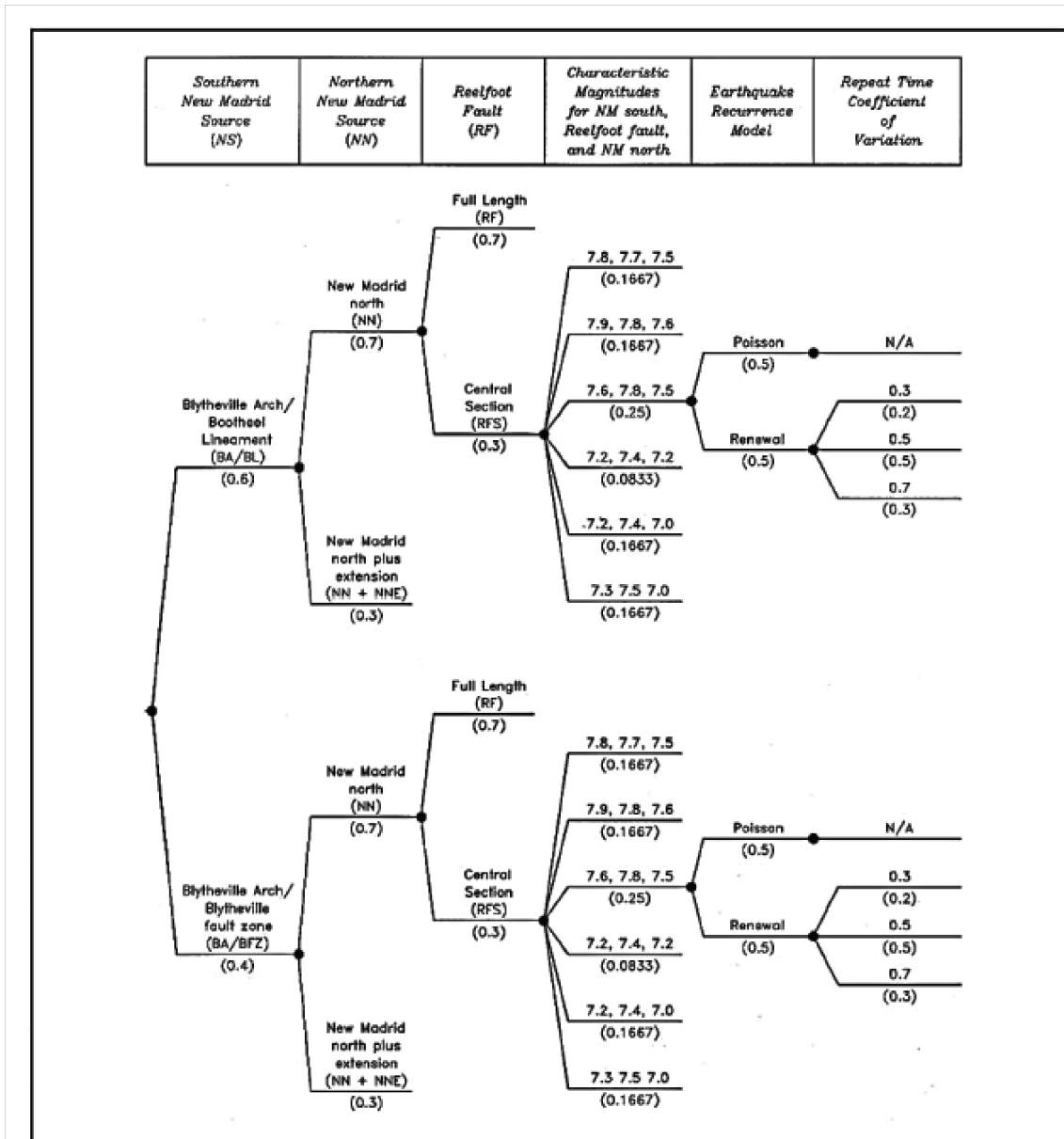
BLN COL 2.5-2

FIGURE 2.5-258
Disaggregation of Hazard from the EPRI-SOG (1988) Seismic Source Model



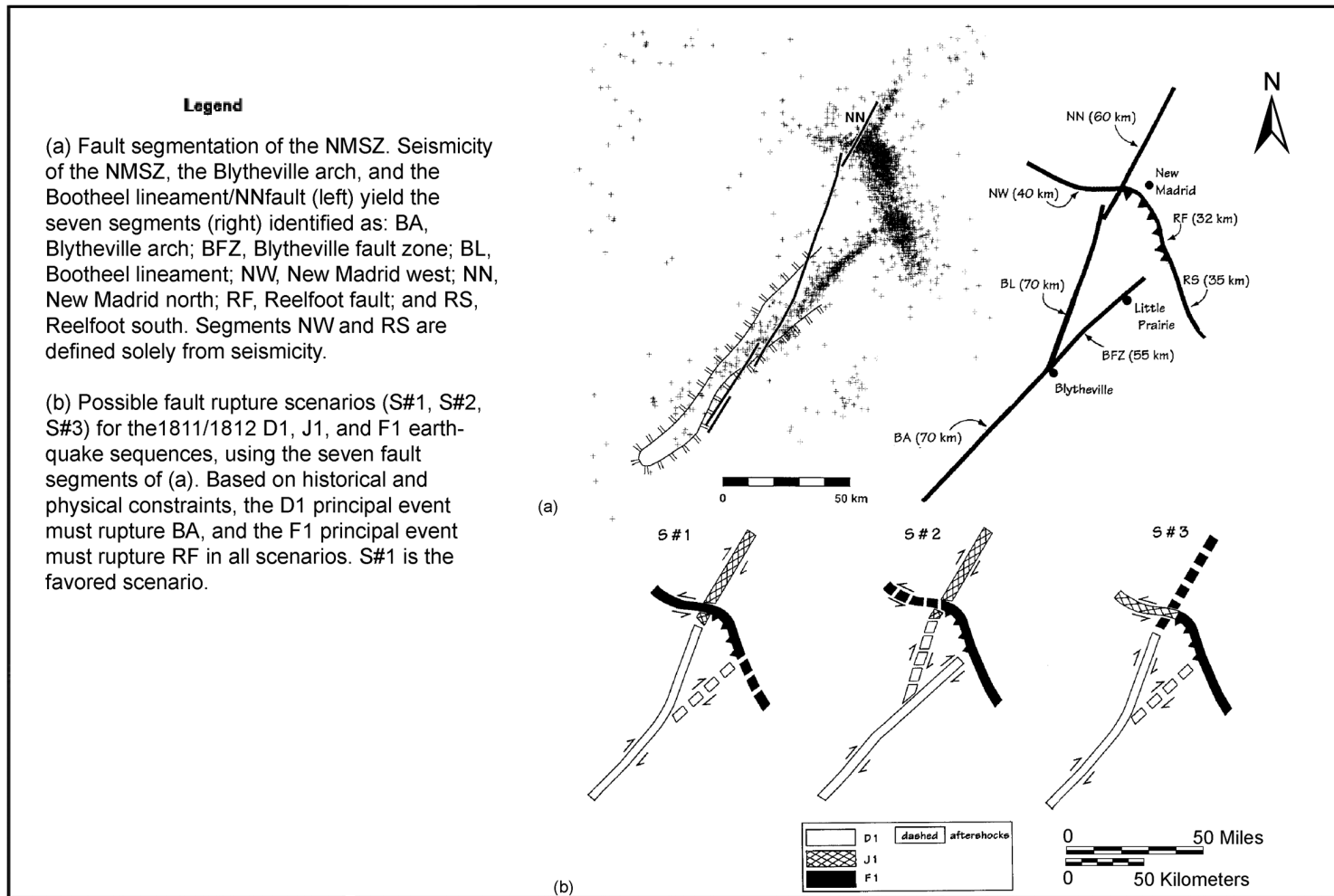
BLN COL 2.5-2

FIGURE 2.5-262
New Madrid (Inset A) and Charleston (Inset B) Repeating Large Magnitude Earthquake Sources



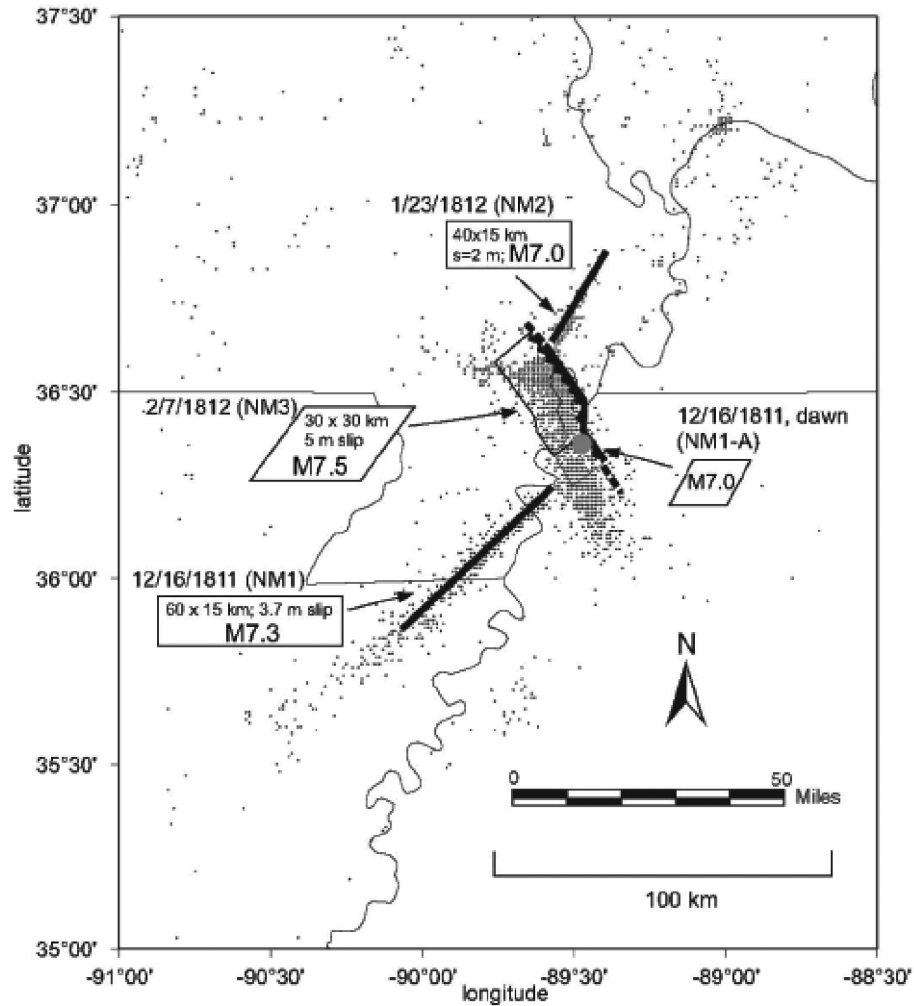
BLN COL 2.5-2

FIGURE 2.5-263
 Source Characterization Logic Tree for Repeating Large Magnitude New Madrid Earthquakes



BLN COL 2.5-2

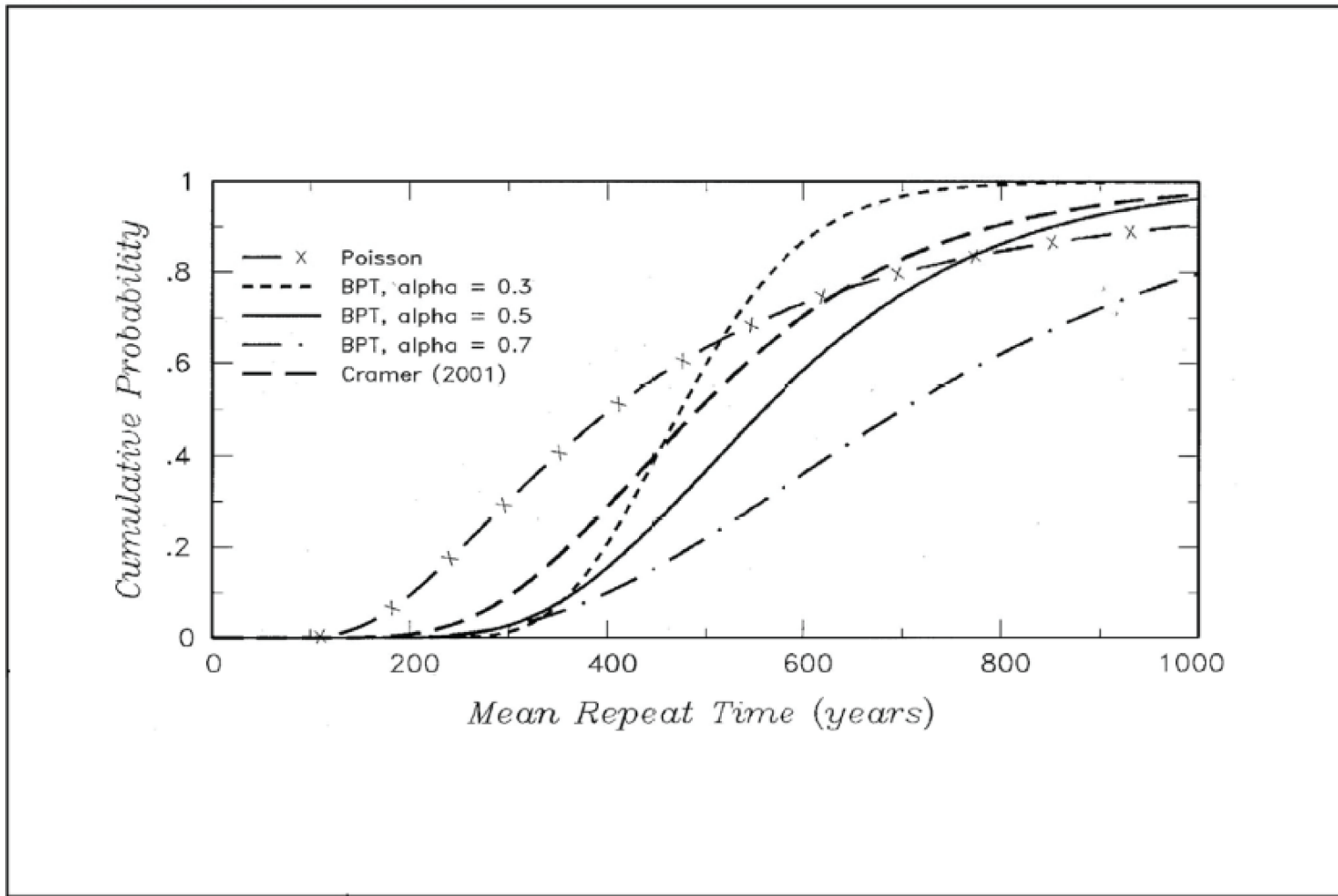
FIGURE 2.5-264
Central Fault System of New Madrid Seismic Zone



(Reference 373)

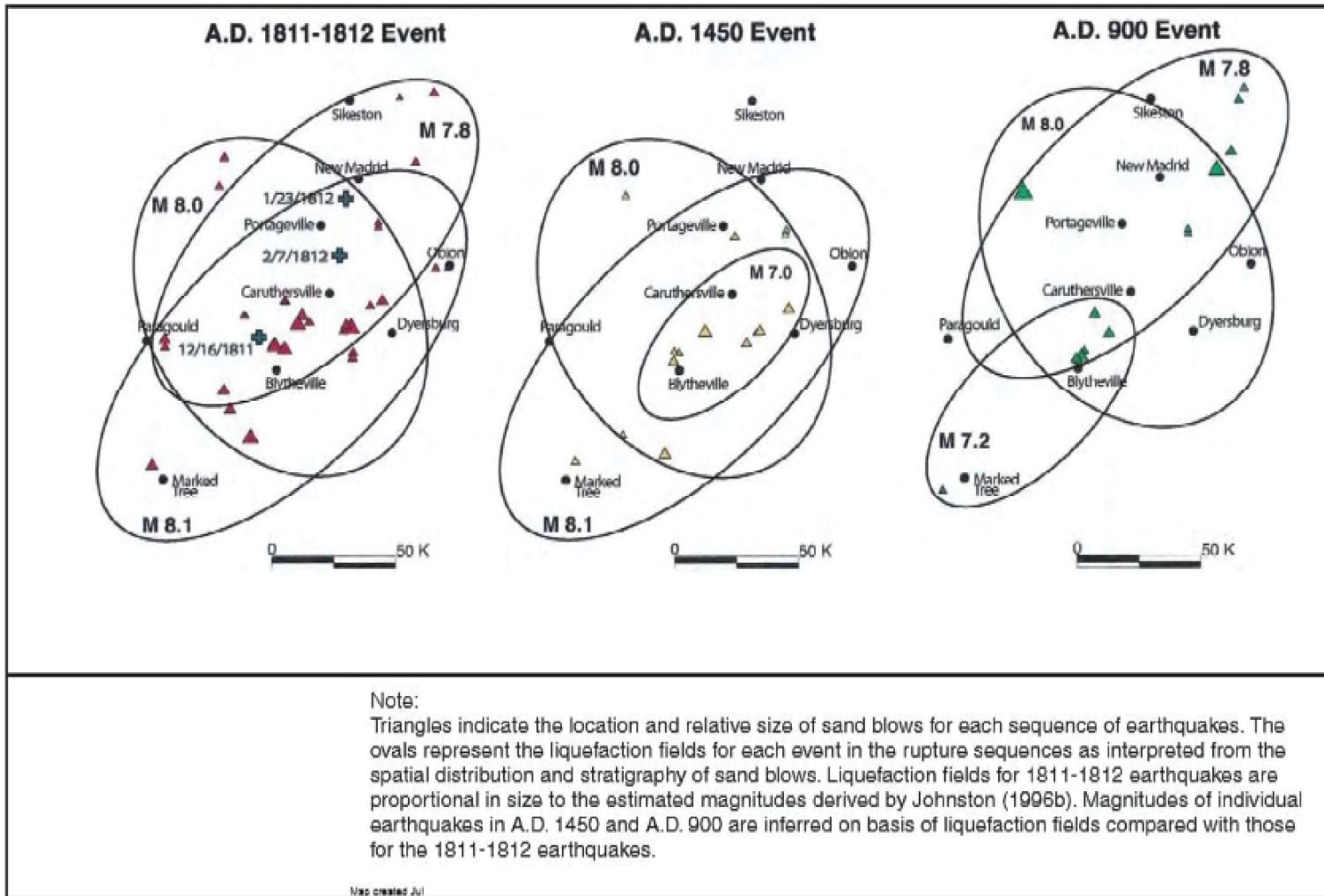
BLN COL 2.5-2

FIGURE 2.5-265
Map Showing Location of New Madrid Seismic Zone as
Illuminated by Seismicity Between 1974 and 1996



BLN COL 2.5-2

FIGURE 2.5-266
Distributions for Mean Repeat Time for New Madrid Repeating Large Magnitude Earthquakes



(References 374 and 297)

BLN COL 2.5-2

FIGURE 2.5-267
 Earthquake Rupture Sequences for Repeating Large Magnitude New Madrid Earthquakes